General Disclaimer

One or more of the Following Statements may affect this Document

- This document has been reproduced from the best copy furnished by the organizational source. It is being released in the interest of making available as much information as possible.

- This document may contain data, which exceeds the sheet parameters. It was furnished in this condition by the organizational source and is the best copy available.

- This document may contain tone-on-tone or color graphs, charts and/or pictures, which have been reproduced in black and white.

- This document is paginated as submitted by the original source.

- Portions of this document are not fully legible due to the historical nature of some of the material. However, it is the best reproduction available from the original submission.

PLASTICITY AND THE CRACK OPENING DISPLACEMENT IN SHELLS

by

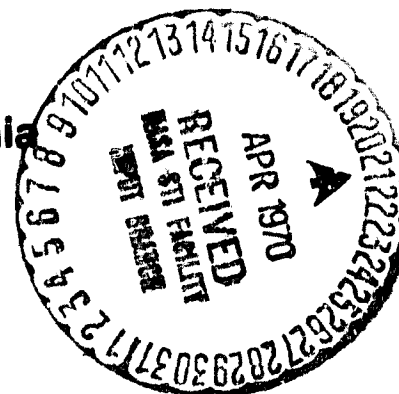F. Erdogan and M. Ratwani

Lehigh University
Bethlehem, Pennsylvania

April 1970

Plasticity and the Crack Opening
Displacement in Shells

by

F. Erdogan and M. Ratwani

Lehigh University
Bethlehem, Pennsylvania

April 1970

Plasticity and the Crack Opening
Displacement in Shells[*]

F. Erdogan and M. Ratwani
Department of Mechanical Engineering and Mechanics,
Lehigh University, Bethlehem, Pennsylvania

Abstract

The plastic deformations and the crack opening displacement,
δ, in cylindrical shells with an axial or circumferential crack
and spherical shells with a meridional crack are considered.
It is assumed that outside the perturbation zone of the crack
the shell is subjected to uniform membrane loads perpendicular
to the crack. The plastic strip model is used to calculate the
plastic zone size. The crack opening displacement is calculated
as the crack surface displacement at the crack tips by using
the conventional superposition technique. In cylindrical shells
with an axial crack the crack surface displacement perpendicular
to the shell surface (i.e., the bulging) is also evaluated.
The results are applied to a set of existing experimental data
on the fracture of cylindrical shells. The tentative conclusion
is that in dealing with the fracture of thin-walled structures,
among various fracture models δ = constant appears to be the
most satisfactory criterion.

Symbols

$2a$:	crack length
$a_p = a + p$	
A_m, A_b, B_{ij}:	stress intensity factor ratios
$c_1 = N_o a_p/(hE)$	
$c_N = N a_p/(hE)$	
$c_M = 6M a_p/(Eh^2)$	
$c_W = \lambda^2 R N_o/(2Eh)$	
$d = a\sigma_Y/E$	
E, ν:	elastic constants
F:	stress function
h:	shell thickness
k^m, k^b:	membrane and bending components of the stress intensity factor
$k = k^m + k^b$	
k_p:	plasticity corrected stress intensity factor
N_{ij}, M_{ij}, $(i,j) = (x,y,z)$:	stress and moment resultants
N_o:	membrane load perpendicular to the crack
N, M:	tractions in the plastic zone
p:	the plastic zone size
R:	mean radius of the shell
u, v, w:	x, y, z- components of the displacement vector
u_1, u_2:	auxiliary functions

x, y, z: dimensionless coordinates

$\alpha = a/a_p$

δ: crack opening displacement

$\lambda = [12(1-\nu^2)]^{1/4} a/(Rh)^{1/2}$: shell parameter

$\lambda_p = [12(1-\nu^2)]^{1/4} \cdot$

$\cdot a_p/(Rh)^{1/2}$

σ_Y: yield strength

1. Introduction

Within the past decade or so the so-called linear fracture
mechanics has established itself as a very satisfactory theo-
retical working tool in studying the phenomena of fatigue crack
propagation and brittle fracture in structural solids. The
theories of fracture or the failure criteria based on the use
of the stress intensity factor, K, or, its equivalent, the
crack extension force, $\mathcal{G}$, have been most effective in cases
for which the size of the plastically deformed region around
the fracture front is small compared to the length parameter
characterizing the fracture area. Thus, the application of
these theories to plane strain fracture and high cycle fatigue
crack propagation involves no ambiguity. However, in the
presence of moderately large plastic deformations, the models
need some re-interpretation or modification. Generally, such
a modification is accomplished by either assuming an increased
crack length (usually by adding the plastic zone size to the

actual crack length) for the purpose of evaluating K or $\mathcal{G}$ [1], or by introducing the concept of "crack opening displacement" [2].

An estimate of the plastic zone size necessary for the application of the first method may be obtained by using the plastic strip model introduced by Dugdale [3] (see also, [4] and [5])[*]. Justification of the widespread use of this modification lies not in the soundness of the underlying physical arguments but primarily in the fact that, in most cases involving the fracture of materials with high toughness, it seems to work, the exceptions being the extreme plane stress configurations.

There is a certain amount of diversity and some confusion involving the definition and the use of the crack opening displacement. However, the most widely accepted definition of it is the relative displacement between the opposing surfaces of the crack at the location corresponding to the actual crack tip obtained from the solution in which the leading edge of the crack is assumed to be at the elastic-plastic boundary. In

---

[*]In [1] and in his subsequent work, Irwin obtained the plastic zone size as the distance from the crack tip to the point at which the cleavage stress is equal to the yield strength of the material. To calculate the cleavage stress the asymptotic relation for small r around the crack tip was used, which gives the plastic zone size as a function of K and yield strength only.

Irwin's simple analysis this corresponds to the relative crack surface displacement at a distance r_y from the crack tip, r_y being the estimate of the plastic zone size. In [5-7] the crack opening displacement was assumed to be the relative crack surface displacement at the (actual) crack tip obtained from the solution based on the plastic strip model.

The differences between the results obtained by using various modifications of the original Griffith-Irwin-Orowan model mentioned above are insignificant if the plastic zone size is relatively small compared to the crack length. However, they become increasingly more noticeable as the relative size of the plastic zone becomes larger. At present, even though far from being perfect, these models seem to be the only satisfactory theoretical tools available and are being rather widely used in practice. Since most of the experimental work in this area has been on mode I type fracture under simple plane loadings, the effectiveness of these models in their applications to fractures under relatively complex combined loading conditions has not yet been tested. In this paper we will treat one such case, namely, the internally pressurized cylindrical or spherical shells with a crack, in which, in addition to the curvature-induced magnification in the stress intensity factor, around the crack the shell is subjected to bending as well as the membrane stresses. The particular geometries which will be considered are the circular cylinder with a longitudinal or a circumferential crack and the spherical shell with a meridional crack.

By using the plastic strip model we will first obtain the plastic zone size, and then from this solution we will calculate the crack opening displacement. Expressions for the displacement component perpendicular to the shell surface (i.e., bulging) will also be developed. The results will then be used to analyze the experimental data given in [8].

2. The Plastic Zone Size

Let the (actual) crack length in the shell be 2a, and the plastic deformations be confined to a narrow strip of length p ahead of the crack tips (Figure 1d). Define

$$a_p = a + p, \quad \alpha = \frac{a}{a_p} \tag{1}$$

To determine the unknown constant a_p (or p) the standard procedure of removing the stress singularities at the fictitious crack tip a_p through the superposition of two solutions will be followed. For simplicity here we will assume that outside the perturbation zone of the crack, the shell is subjected to symmetrically applied constant membrane stresses and in this region the stress resultant which is perpendicular to the crack is N_o.

Defining the shell parameters

$$\lambda = [12(1-\nu^2)]^{1/4} a/(Rh)^{1/2}, \quad \lambda_p = [12(1-\nu^2)]^{1/4} a_p/(Rh)^{1/2} \tag{2}$$

-6-

we first obtain the solution for a shell with a crack of length $2a_p$ and subjected to the membrane load $N_y = -N_o$. This solution gives the membrane and bending components of the stress intensity factor as follows [9]:

$$k_1^m = A_m(\lambda_p)N_o \frac{\sqrt{a_p}}{h}, \quad k_1^b = A_b(\lambda_p)N_o \frac{\sqrt{a_p}}{h} \qquad (3)$$

where the stress intensity factor ratios A_m and A_b are functions of λ_p only and are obtained numerically in tabular form.

We next consider the shell solution under the external loads coming from the plastic strips lying ahead of the crack tips. For this we will assume that the crack length again is $2a_p$ and the shell is subjected to the following surface tractions at the crack surfaces[*]:

$$N_y = N, \quad M_y = M, \quad \alpha < |x| < 1$$

$$N_y = 0, \quad M_y = 0, \quad |x| < \alpha \qquad (4)$$

$$N_{xy} = 0, \quad V_y = 0, \quad |x| < 1$$

As in most applications of the plastic strip model, here we will

_____

[*] Here x, y, z are the dimensionless rectangular coordinates with the origin at the mid point of the crack, x is directed along the crack and z is directed inward perpendicular to the shell surface (see Figure 1). The non-dimensionalizing length parameter is a_p.

assume that the unknown tractions N and M are constant. The solution of this problem gives the stress intensity factors as (see the Appendix),

$$k_2^m = B_{11}(\alpha,\lambda_p)N\,\frac{\sqrt{a_p}}{h} + B_{12}(\alpha,\lambda_p)M\,\frac{6\sqrt{a_p}}{h^2}$$

$$(5)$$

$$k_2^b = B_{21}(\alpha,\lambda_p)N\,\frac{\sqrt{a_p}}{h} + B_{22}(\alpha,\lambda_p)M\,\frac{6\sqrt{a_p}}{h^2}$$

where the stress intensity factor ratios B_{ij} ($i,j = 1,2$) are calculated in tabular form as functions of α and λ_p.

The condition that the stress intensity factors should vanish at $x = \mp 1$ (i.e., at the ends of the plastic zone) may now be expressed as

$$k_1^m + k_2^m = 0, \quad k_1^b + k_2^b = 0 \qquad (6)$$

Or, by using (3) and (5) and dividing by the yield strength, σ_Y, we find

$$B_{11}\,\frac{N}{h\sigma_Y} + B_{12}\,\frac{6M}{h^2\sigma_Y} + A_m\,\frac{N_o}{h\sigma_Y} = 0$$

$$(7)$$

$$B_{21}\,\frac{N}{h\sigma_Y} + B_{22}\,\frac{6M}{h^2\sigma_Y} + A_b\,\frac{N_o}{h\sigma_Y} = 0$$

In the plastic strip, $\alpha < |x| < 1$, the tractions N and M are expected to satisfy some kind of a yield condition. One such condition which is most commonly used may be expressed as

$$\frac{N}{h\sigma_Y} + \left| \frac{6M}{h^2\sigma_Y} \right| = 1 \qquad (8)$$

Equations (7) and (8) provide three (highly nonlinear) algebraic equations to determine the unknowns α, N and M. Once α is determined, (1) gives the plastic zone size p as

$$p = a\left(\frac{1}{\alpha} - 1\right) \qquad (9)$$

Eliminating N and M, (7) and (8) may be put in the following form:

$$[(b_{11}+b_{21})A_m + (b_{12}+b_{22})A_b] \frac{N_0}{h\sigma_Y} + 1 = 0 \qquad (10)$$

where the matrix (b_{ij}) is the inverse of (B_{ij}) (which is assumed to be non-singular). Noting that $\lambda_p = \lambda/\alpha$, (10) determines α as a function of the (actual) shell parameter λ and the stress ratio $N_0/h\sigma_Y$. For the limiting case $\lambda = 0$, the problem is that of uniformly loaded flat plate and α is given by

$$\alpha = \cos \frac{\pi N_0}{2h\sigma_Y}, \quad (\lambda = 0) \qquad (11)$$

For the three geometries under consideration the solution of (10) is shown in Figures 2-4. Comparison of the results

-9-

given in [9] and [13] indicates that the effect of curvature on the stress intensity factor in cylindrical shells with a circumferential crack is small compared to that in cylindrical shells with an axial crack and spherical shells with a meridional crack. As seen from Figures 2-4, this trend is also valid for plastic zone size. As the stress ratio $N_0/h\sigma_Y$ increases, the convergence of the numerical procedure becomes slower, and more computer time is required to calculate the α values. This is the reason for seemingly incomplete plots in the Figures.

Obviously, it would be desirable to have analytical expressions for α as a function of $N_0/h\sigma_Y$ which are acceptable approximations. For the cylindrical shell with a circumferential crack the expression

$$\alpha = (\cos \frac{\pi N_0}{2h\sigma_Y})^{1 + 0.2\lambda} + 0.00854\lambda \ e^{-\lambda^3} \sin \frac{\pi N_0}{h\sigma_Y} \qquad (12)$$

seems to be quite satisfactory except for the range in which both λ and $N_0/h\sigma_Y$ are large ($\lambda > 3$, $N_0/h\sigma_Y > 0.7$). To obtain a similar degree of accuracy in representing the results of the other two geometries, the expressions become much too cumbersome to be practical; hence, are not included in this paper.

3. The Crack Opening Displacement

Referring to Figure 1, to obtain the crack opening displacement, the y-component of the displacement vector on the

crack surface (at the middle surface of the shell), $v(x,o)$, has to be calculated. This is obtained from

$$\epsilon_y = \frac{1}{Eh} (N_y - \nu N_x) = \frac{\partial v}{a_p \partial y} - \frac{w}{R_y} \tag{13}$$

where a_p is the half-crack length which is used to normalize the dimensions, w is the z-component of the displacement vector, and R_y is the principal radius of curvature in y-z plane. In terms of the stress function F and the displacement w, (13) may be expressed as

$$\frac{\partial v}{\partial y} = \frac{1}{Eha_p} (\frac{\partial^2 F}{\partial x^2} - \nu \frac{\partial^2 F}{\partial y^2}) + \frac{a_p}{R_y} w \tag{14}$$

For the cylindrical shell with a circumferential crack $R_y = \infty$ and the analysis is much simpler than the other two cases. For this case, the displacement at the crack surface is found as (see the Appendix)

$$v(x,o) = \frac{2ia_p}{\lambda_p^2 R} [(1-\nu)u_1(x) + (1+\nu)u_2(x)], \quad |x| < 1 \tag{15}$$

where u_1 and u_2 are the auxiliary functions obtained from the solution of the integral equations (A1) mentioned in the Appendix.

For the cylindrical shell with an axial crack $R_y = R$ is the mean radius of curvature of the cylinder. Thus, expressing F and w in terms of the functions $u_i(x)$ and following a procedure similar to that outlined in the Appendix, from (14),

-11-

after some lengthy manipulations, the crack surface displacement may be obtained as[*]

$$v(x,o) = \begin{cases} - \dfrac{2ia_p}{R\lambda_p^2} [(2-\nu)u_1(x) - \nu u_2(x)], & |x|<1 \\ \\ 0, & |x|>1 \end{cases} \qquad (16)$$

In the case of the spherical shell the result does not come out to be as simple as that given by (15) and (16). It involves repeated indefinite integrals of u_1 and u_2, and requires elaborate numerical work for its evaluation. Since the numerical work was not completed, in this paper we will not include any results concerning the crack opening displacement in spherical shells.

When the plastic strip model is used to account for yielding around the crack tips, the crack opening displacement will be defined as the relative crack opening at $x = \mp \alpha$ obtained from the superposition of the following two solutions:

1. The shell with crack length $2a_p$ subjected to the tractions (Figure 1d)

$$N_y = -N_o, \quad M_y = 0, \quad N_{xy} = 0, \quad V_y = 0, \quad (|x|<1, \ y = 0) \qquad (17)$$

---

[*]The integration constant coming from (14) is determined from the condition that $v(\mp 1,0) = 0$.

2. Same shell subjected to the tractions given by (4)
   where α, N and M satisfy conditions (7) and (8). Thus,
   the crack opening displacement δ may be expressed as

$$\delta = 2[v_1(\alpha,o) + v_2(\alpha,o)] \tag{18}$$

where, for convenience, we may also write

$$v_2(\alpha,o) = v_{2N} + v_{2M}$$

v_{2N} and v_{2M} being the individual contributions of the
loads N and M, respectively.

Figures 5, 6 and 7 show some calculated results for the
crack surface displacement v. In Figures 5 and 7, the solid
curves simply represent the displacement $v(x,o)$, $|x|<1$, in a
shell with the parameter λ_p and subjected to the uniform mem-
brane load $N_y = -N_0$ along $|x|<1$. The dashed curves v_{2N} shown
in these figures are, on the other hand, obtained as the dis-
placement at $x = \alpha$ from a solution in which $N_y = N$ applied
along $\alpha < |x| < 1$, $y = 0$ is the only external load. Similarly,
in Figure 6, the solid and dashed curves, v_M/c_M and v_{2M}/c_M,
are, respectively, obtained from the external loads $M_y = M$,
$|x|<1$, and $M_y = M$, $\alpha<|x|<1$. The length parameters shown in
the figures which are used to non-dimensionalize v_1, v_{2N} and
v_{2M} are, respectively, given by

$$c_1 = \frac{N_o a_p}{hE}, \quad c_N = \frac{N a_p}{hE}, \quad c_M = \frac{6M a_p}{Eh^2} \tag{19}$$

In the case of circumferential crack, since the relative magnitude of the bending moment M and its effect on α and δ were extremely small, for this geometry the moment-induced displacements similar to that of Figure 6 are not presented.

The results given in Figures 5-7, with Figures 2 and 4, may be considered as a set of master curves from which the crack opening displacement δ can be calculated as a function of λ and $N_o/(h\sigma_Y)$. In fact, it can easily be shown that

$$\frac{\delta}{d} = \frac{2}{\alpha} \left(\frac{N_o}{h\sigma_Y} \frac{v_1}{c_1} + \frac{N}{h\sigma_Y} \frac{v_{2N}}{c_N} + \frac{6M}{h^2\sigma_Y} \frac{v_{2M}}{c_M} \right), \quad d = \frac{a\sigma_Y}{E} \tag{20}$$

where α and the load ratios $N/(\sigma_Y h)$ and $6M/(h^2\sigma_Y)$ are obtained from the plastic strip analysis by solving (7) and (8). α is given in Figures 2-4. For a cylindrical shell with an axial crack, the ratio of the bending stress $6M/h^2$ to the membrane stress N/h applied on the plastic strip $\alpha < |x| < 1$ is shown in Figure 8.

In the limiting case of $\lambda = 0$ (i.e., the flat plate) the crack surface displacement v_1 and the crack opening displacement δ are given by

$$\frac{v_1(x,0)}{c_1} = 2\sqrt{1-x^2}, \quad |x|<1$$

<div align="right">(21)</div>

$$\frac{\delta}{d} = -\frac{8}{\pi}\log(\cos\frac{\pi N_0}{2h\sigma_y})$$

The numerical results for δ obtained from (20) and (21) are shown in Figures 9 and 10.

4. Normal Displacement - Bulging

To give an idea about the nature and the magnitude of the displacement component, w, normal to the shell surface, in this section we will obtain the expression for this displacement at $y = 0$. This will be done only for the cylindrical shell with an axial crack which is subjected to the tractions $N_y = -N_0$ along $|x|<1$, and which, from the practical viewpoint, is the most important case. Referring again to the basic formulation of the problem, at $y = 0$ the displacement w may be expressed in terms of the auxiliary functions u_1 and u_2 as follows:

$$w(x,0^+) = \frac{1}{4\pi}\int_{-1}^{1}[h_1(x,t)u_1(t) + h_2(x,t)u_2(t)]dt \tag{22}$$

where

$$h_1(x,t) = \int_0^\infty [\sum_1^4 \frac{1}{s_i} + \frac{s}{\alpha_1}(\frac{1}{s_1} - \frac{1}{s_2}) - \frac{(3-2\nu)s}{\alpha_2}(\frac{1}{s_3} - \frac{1}{s_4})]\cdot$$
$$\cdot\cos s(t-x)ds$$

$$h_2(x,t) = \int_0^\infty \left[\sum_1^4 \frac{1}{s_i} - \frac{s}{\alpha_1} \left(\frac{1}{s_1} - \frac{1}{s_2} \right) - \frac{(1-2\nu)s}{\alpha_2} \left(\frac{1}{s_3} - \frac{1}{s_4} \right) \right] \cdot$$

$$\cdot \cos s(t-x)ds$$

$$s_1 = \sqrt{s(s-\alpha_1)}, \quad s_2 = \sqrt{s(s+\alpha_1)}, \quad s_3 = \sqrt{s(s-\alpha_2)}, \quad s_4 = \sqrt{s(s+\alpha_2)}$$

$$\alpha_1 = \lambda e^{\pi i/4}, \quad \alpha_2 = \lambda e^{-\pi i/4}$$

The kernels $h_i(x,t)$ may be expressed in terms of the following two types of integrals:

$$\int_0^\infty \left(\frac{1}{s_1} + \frac{1}{s_2} \right) \cos s(t-x)ds = 2\cos\left(\frac{\alpha_1(t-x)}{2}\right) K_0\left(\frac{\alpha_2|t-x|}{2}\right)$$

$$\int_0^\infty s\left(\frac{1}{s_1} - \frac{1}{s_2} \right) \cos s(t-x)ds = \alpha_1 \cos\left(\frac{\alpha_1(t-x)}{2}\right) K_0\left(\frac{\alpha_2|t-x|}{2}\right)$$

$$- \alpha_2 \sin\left(\frac{\alpha_1(t-x)}{2}\right) K_1\left(\frac{\alpha_2(t-x)}{2}\right)$$

Note that h_i has a logarithmic singularity at $x = t$ which requires some special care in evaluating (22). Also note that (22) is valid for $|x| > 1$ as well as for $|x| < 1$.

Figure 11 shows the displacement w evaluated for the shell parameter $\lambda = 2$. The length parameter c_w shown in the figure is given by

$$c_w = \frac{\lambda^2 R N_0}{2Eh}$$

Note that on the crack surface w is calculated to be negative, meaning that the displacement is outward. Also note the slight depression or inward displacement ahead of the crack tip.

5. Application to Experimental Results

It was pointed out that in the presence of plastic deformations around the crack tips, the fracture of the "thin-walled" structure may be analyzed by using either the plasticity-corrected stress intensity factor, k_p, or the crack opening displacement, δ. As an example, in this section we will analyze the data given in [8]. The material used in [8] was 2014-T6 aluminum which was tested at -320°F and -423°F. The dimensions and the yield strength of the cylinders were:

R = 2.81 in., h = 0.06 in., 0.104<2a<2.0 in.

σ_Y = 94,200 psi (at -320°F)

σ_Y = 104,000 psi (at -423°F)

Figures 12 and 13 show the elastic stress intensity factor, $k = k^m + k^b$, and the plasticity-corrected stress intensity factor k_p evaluated by using the results of [9] and this paper[*]. The figures indicate that there is an apparent improvement in the correlation of the data if the plasticity correction is

_____

[*] k_p is calculated by replacing a by $a_p = a + p$ in the elastic analysis.

used (i.e., over the range of crack lengths $0.1 < 2a < 2$ in., k_p is closer to being constant as compared with k). Figure 14 shows the calculated crack opening displacement δ obtained from the same data. Comparing the trend of the data as presented in Figure 14 with that of Figures 12 and 13, $\cdot$ = constant appears to be a more acceptable fracture criterion. Thus, on the basis of this limited experimental verification, one may tentatively conclude that, until a better criterion for plane stress fracture is developed, δ = constant may serve as a satisfactory model.

References

1. G. R. Irwin, "Plastic zone near a crack and fracture toughness", Proc. Sagamore Res. Ord. Materials, p. 63 (1960).

2. A. A. Wells, "Notched bar tests, fracture mechanics and the brittle strengths of welded structures", B. W. J. vol. 12, p. 2 (1962).

3. D. S. Dugdale, "Yielding of steel sheets containing slits", J. Mech. Phys. Solids, vol. 8, p. 100 (1960).

4. G. I. Barenblatt, "Mathematical theory of equilibrium cracks in brittle fracture", Advances in Applied Mechanics, vol. 7, p. 55 (1962).

5. B. A. Bilby, A. H. Cottrell and K. H. Swinden, "The spread of plastic yielding from a notch", Proc. Roy. Soc. A272, p. 304 (1963).

6. B. A. Bilby, A. H. Cottrell, E. Smith and K. H. Swinden, "Plastic yielding from sharp notches", Proc. Roy. Soc. A279, p. 1 (1964).

7. F. Erdogan, "Elastic-plastic anti-plane problems for bonded dissimilar media containing cracks and cavities", Int. J. Solids Structures, vol. 2, p. 447 (1966).

8. R. B. Anderson and T. L. Sullivan, "Fracture mechanics of through-cracked cylindrical pressure vessels", NASA TN D-3252 (1966).

9. F. Erdogan and J. J. Kibler, "Cylindrical and spherical shells with cracks", Int. J. Fracture Mechanics, vol. 5, p. 229 (1969).

10. E. S. Folias, "An axial crack in a pressurized cylindrical shell", Int. J. Fracture Mechanics, vol. 1, p. 104 (1965).

11. E. S. Folias, "A finite line crack in a pressurized spherical shell", Int. J. Fracture Mechanics, vol. 1, p. 20 (1965).

12. E. S. Folias, "A circumferential crack in a pressurized cylindrical shell", Int. J. Fracture Mechanics, vol. 3, p. 1 (1967).

13. F. Erdogan and M. Ratwani, "Fatigue and fracture of cylindrical shell containing a circumferential crack", to appear in Int. J. Fracture Mechanics (1970).

APPENDIX

Integral Equations

The solution of the problems for symmetrically loaded cylindrical and spherical shells containing a crack can be reduced to that of a system of singular integral equations of the following form [9-13]:

$$\int_{-1}^{1} \sum_{1}^{2} a_{ij} u_j(t) \frac{dt}{t-x} + \int_{-1}^{1} \sum_{1}^{2} k_{ij}(x,t) u_j(t) dt = f_i(x)$$

(A1)

$$i = 1,2, \quad |x| < 1$$

where, for the three basic geometries considered in this paper, the coefficients a_{ij} are known constants and the kernels k_{ij} are bounded known functions. The functions f_i are given in terms of crack surface tractions as follows[*]

$$f_1(x) = \frac{\pi \lambda^2 R}{iEh} \int_0^x N_y(x) dx$$

(A2)

$$f_2(x) = \frac{\pi a^2}{D} \int_0^x M_y(x) dx, \quad D = Eh^3/[12(1-\nu^2)]$$

Once the auxiliary functions u_i are determined, all the field quantities in the shell, such as displacements, stress result-

---

[*]Note that, through a suitable superposition, the singular portion of the problem can always be reduced to one in which crack surface tractions are the only external loads.

-20-

ants or moment resultants, may be expressed in terms of definite integrals of u_1 and the kernels corresponding to the particular field quantity.

In the calculation of the plastic zone size, the stress intensity ratios $A_m(\lambda_p)$ and $A_b(\lambda_p)$ shown in equation (3) were obtained by letting $N_y = - N_0$ and $M_y = 0$ in (A2) and by following the procedure outlined in [13] and [9]. For the calculation of B_{ij} shown in (5), the tractions are given by (4). Thus the input functions become:

$$f_1(x) = \begin{cases} 0, & |x| < \alpha \\[2em] \dfrac{\pi \lambda_p^2 R}{1Eh} N(x-\alpha), & \alpha < |x| < 1 \end{cases}$$

$$\text{(A3)}$$

$$f_2(x) = \begin{cases} 0, & |x| < \alpha \\[2em] \dfrac{\pi a^2}{D} M(x-\alpha), & \alpha < |x| < 1 \end{cases}$$

Crack Opening Displacement
=======

To give an idea about the procedure followed to evaluate the crack opening displacements, here we will briefly consider the problem of a cylindrical shell with a circumferential crack

which, in this respect, is the simplest of the three problems considered in this paper. Let u, v, w refer to the x, y, z components of the displacement vector and let x and z be, respectively, directed along the crack and perpendicular to the tangent plane of the shell (Figure 1). Hence the displacement of interest is v, which can be expressed as

$$\frac{\partial v}{a \partial y} = \epsilon_y = \frac{1}{hE} (N_y - \nu N_x) = \frac{1}{a^2 Eh} \left(\frac{\partial^2 F}{\partial x^2} - \nu \frac{\partial^2 F}{\partial y^2} \right) \tag{A4}$$

where F is the stress function. Referring to [12] and [13] and integrating* (A4), after some lengthy manipulations we obtain

$$\frac{\lambda^2 R}{2ia} v(x,o) = \int_0^\infty [(1-\nu)(P_1+P_2)(s^2+\lambda i/2)^{1/2}$$

$$+ (1+\nu)(P_1-P_2) \frac{\lambda}{2} e^{\pi i/4}]\cos xs ds \tag{A5}$$

Considering the following definition of u_1 and u_2

$$\int_0^\infty (P_1+P_2)(s^2+\lambda i/2)^{1/2}\cos xs ds = \begin{cases} u_1(x), & |x|<1 \\ 0, & |x|>1 \end{cases}$$

$$\tag{A6}$$

$$\int_0^\infty (P_1-P_2) \frac{\lambda}{2} e^{\pi i/4}\cos xs ds = \begin{cases} u_2(x), & |x|<1 \\ 0, & |x|>1 \end{cases}$$

*The integration "quantity" arising from (A4) is a constant and is determined from $v(\pm 1, 0) = 0$.

(A5) simply becomes

$$\frac{\lambda^2 R}{2\mu a} \, v(x,o) = \begin{cases} (1-\nu)u_1(x) + (1+\nu)u_2(x), & |x| < 1 \\ \\ 0, & |x| > 1 \end{cases} \tag{A7}$$

where $v(x,o)$ is one-half of the crack opening displacement.
The unknown functions u_1 and u_2 are obtained from the solution
of (A1).
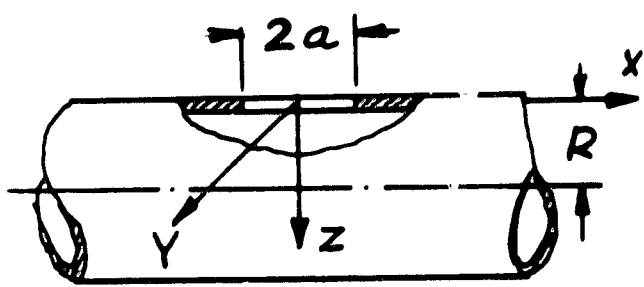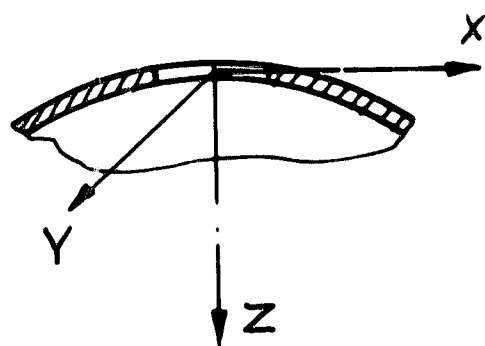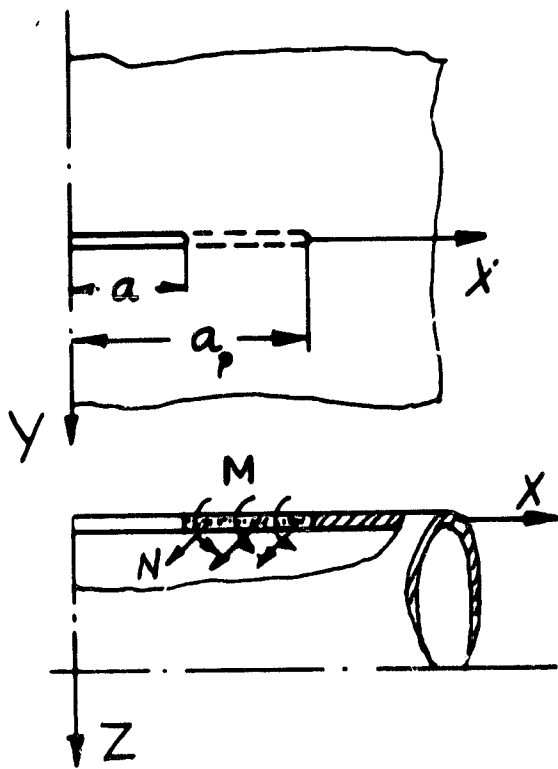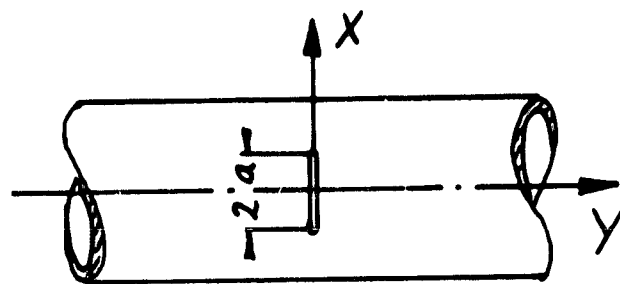
Figure 1. The crack geometries.
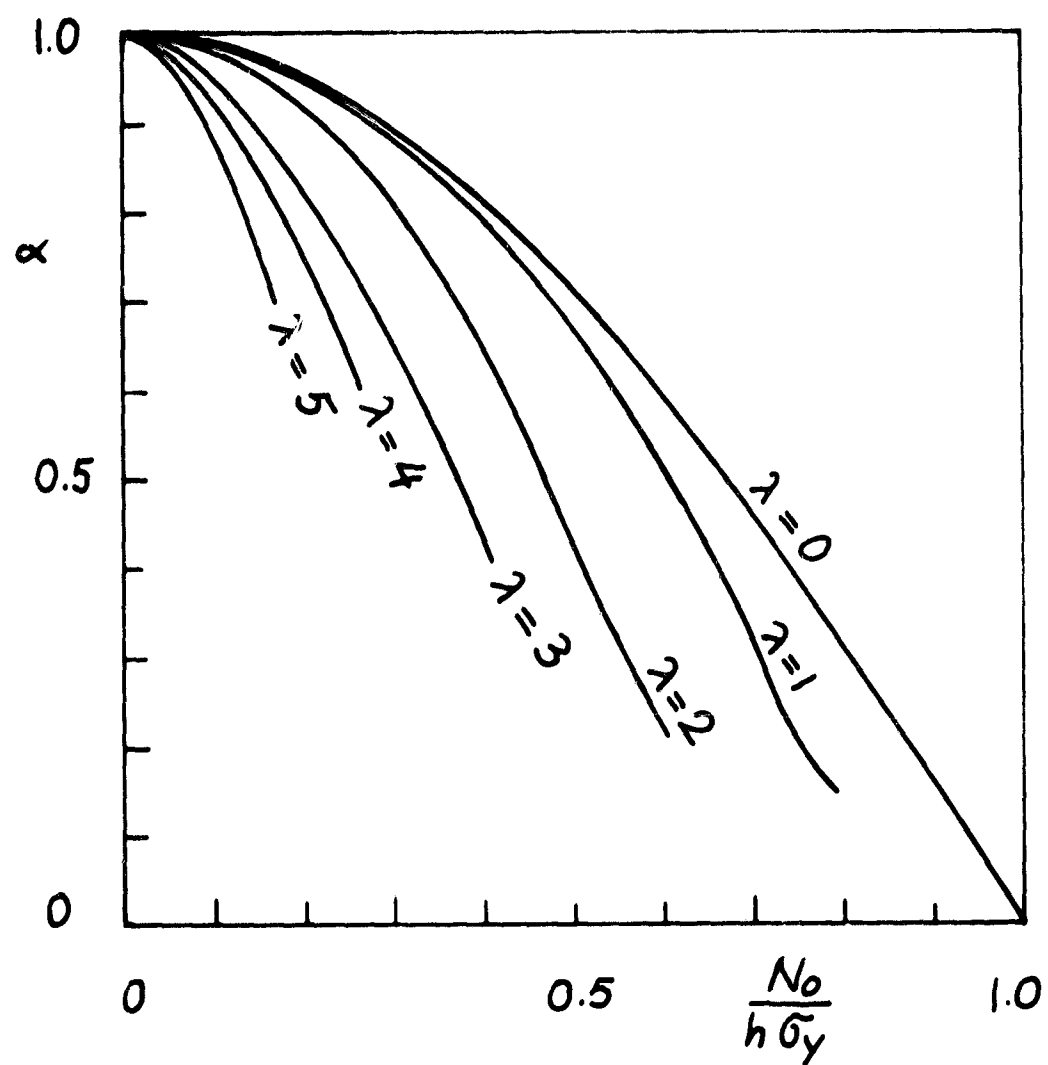
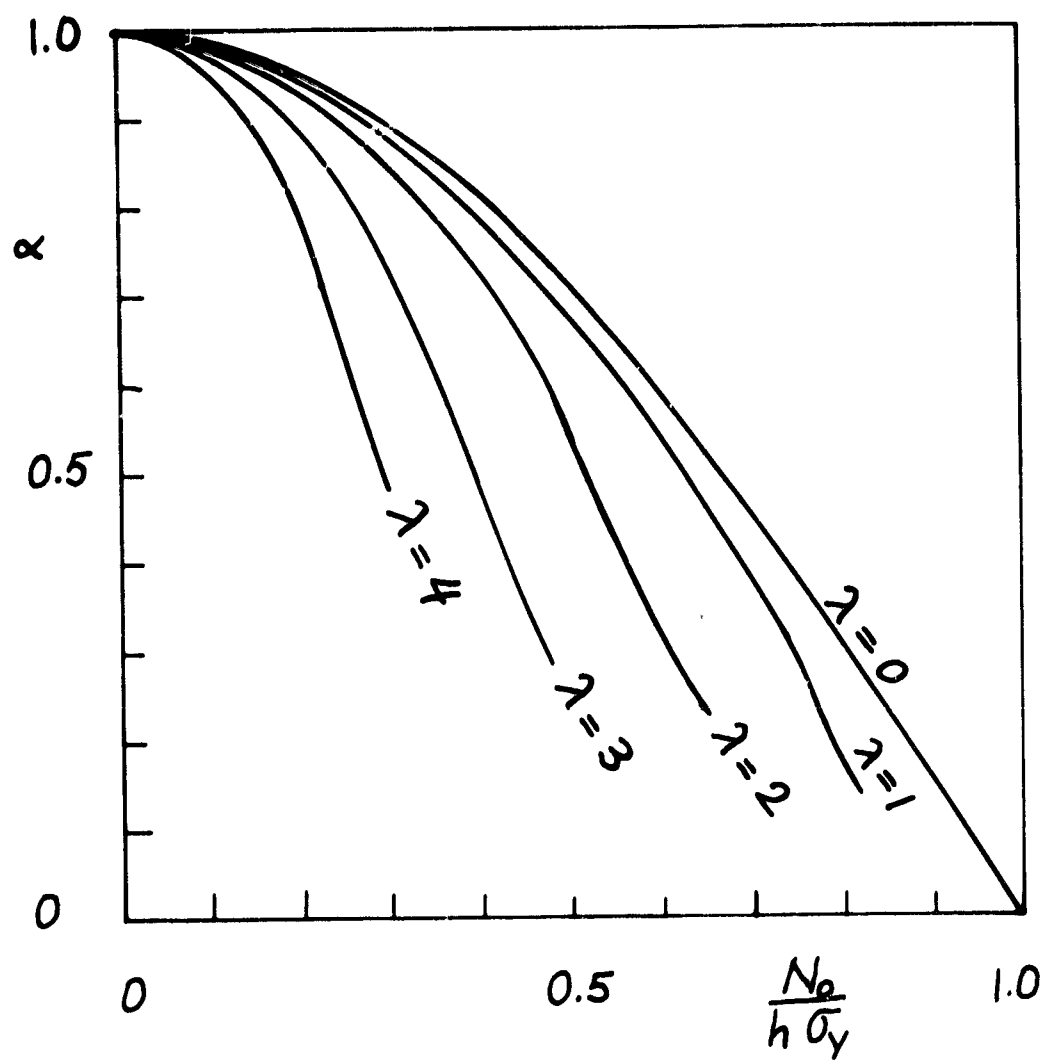Figure 2. The plastic zone factor α vs. the load ratio $N_o/(h\sigma_Y)$ in cylindrical shells with an axial crack.

Figure 3. α vs. $N_0/(h\sigma_y)$ in spherical shells with a meridional crack.
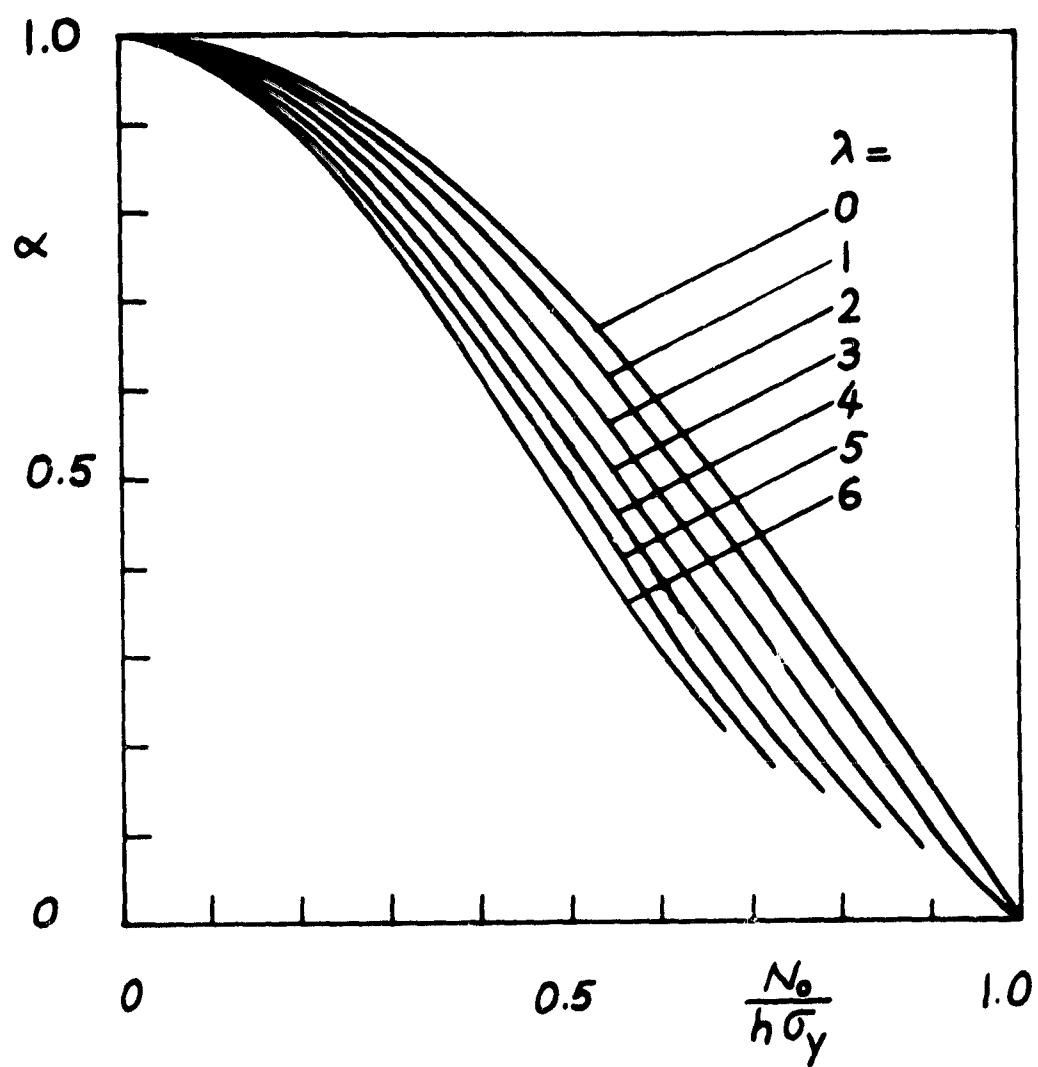
Figure 4. α vs. $N_0/(h\sigma_Y)$ in cylindrical shells with a circumferential crack.
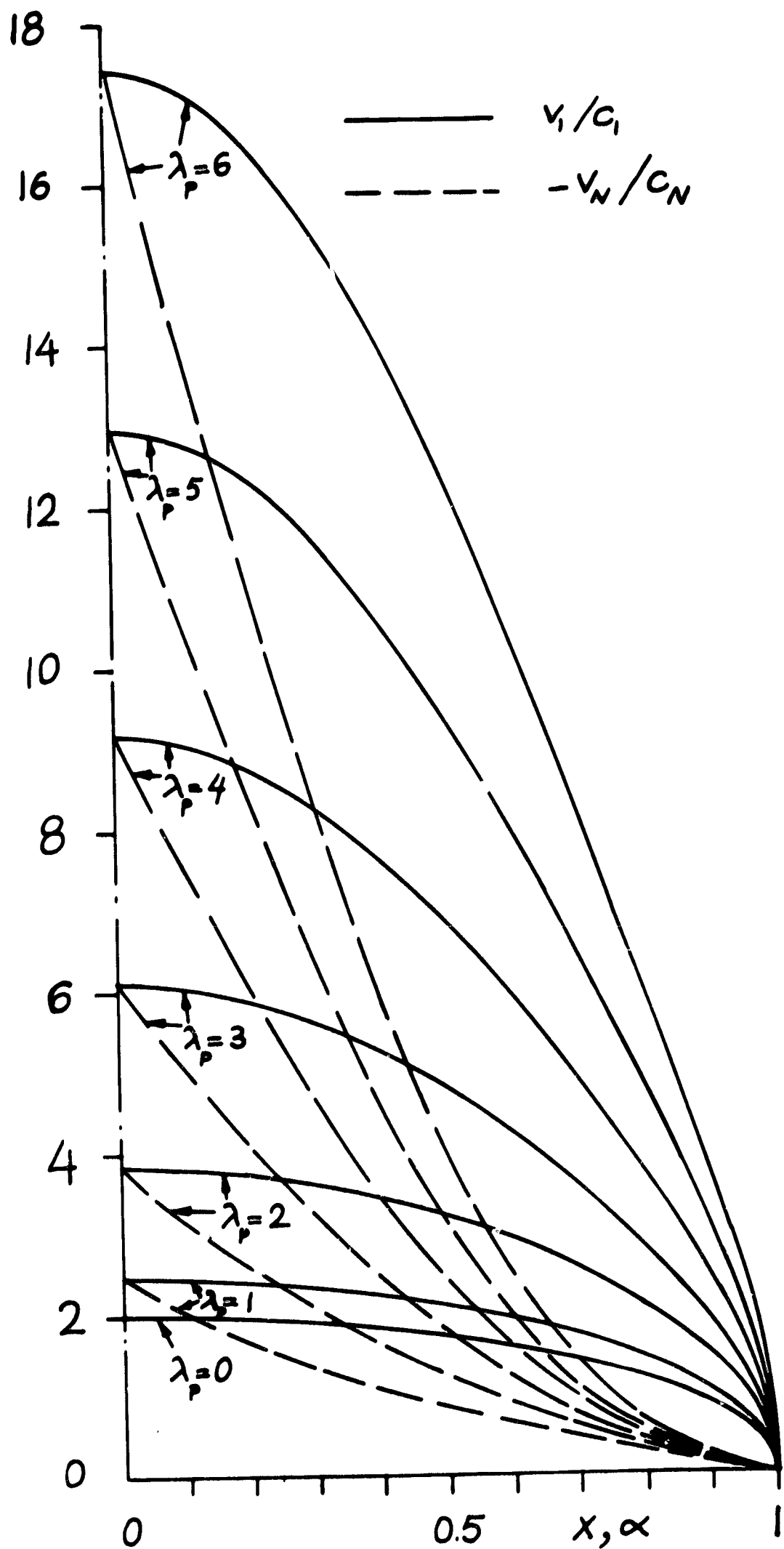
Figure 5. Crack surface displacements in cylindrical shells with an axial crack under membrane loads.
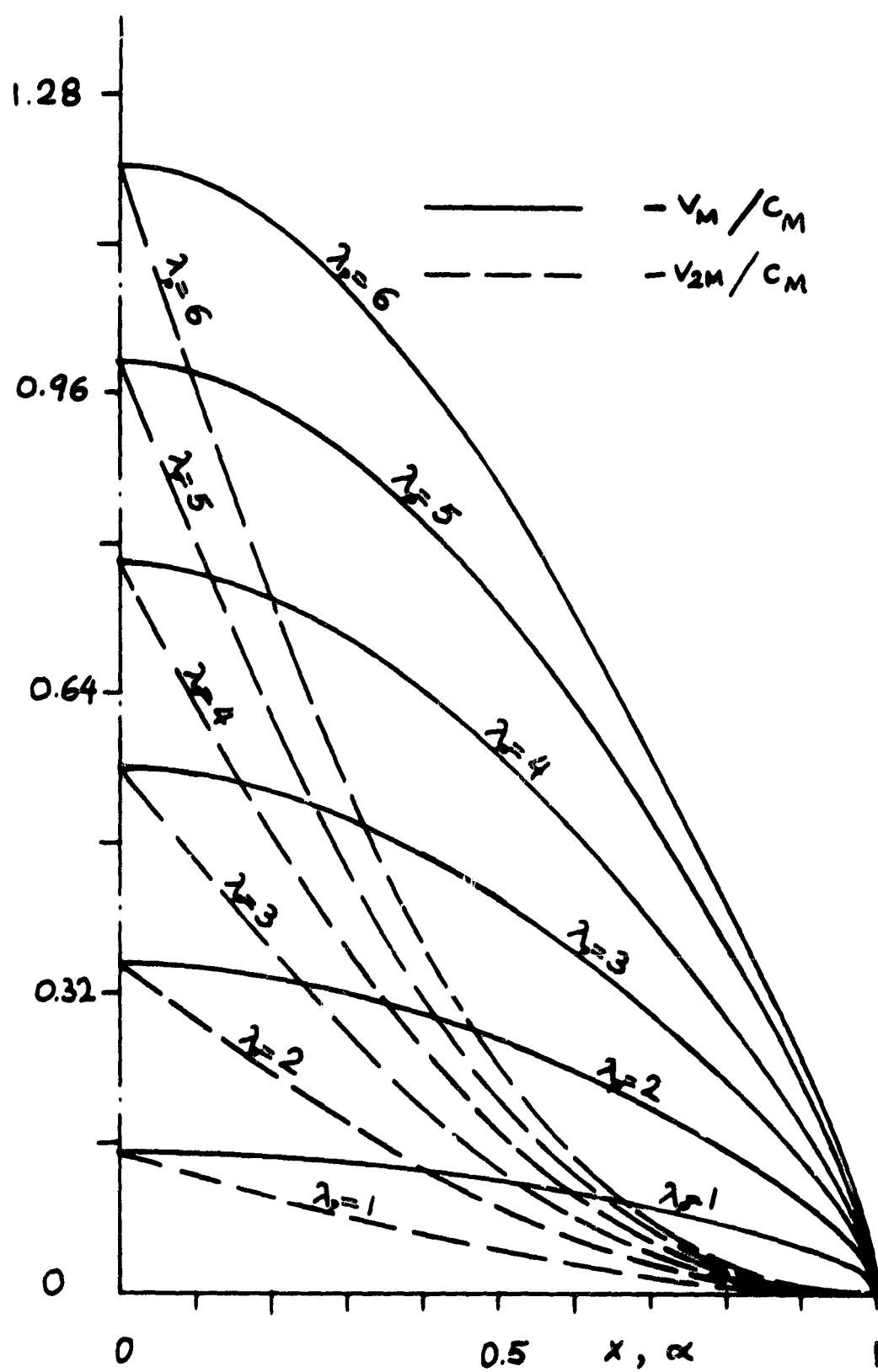
Figure 6. Crack surface displacements in cylindrical shells
with an axial crack under bending moments.
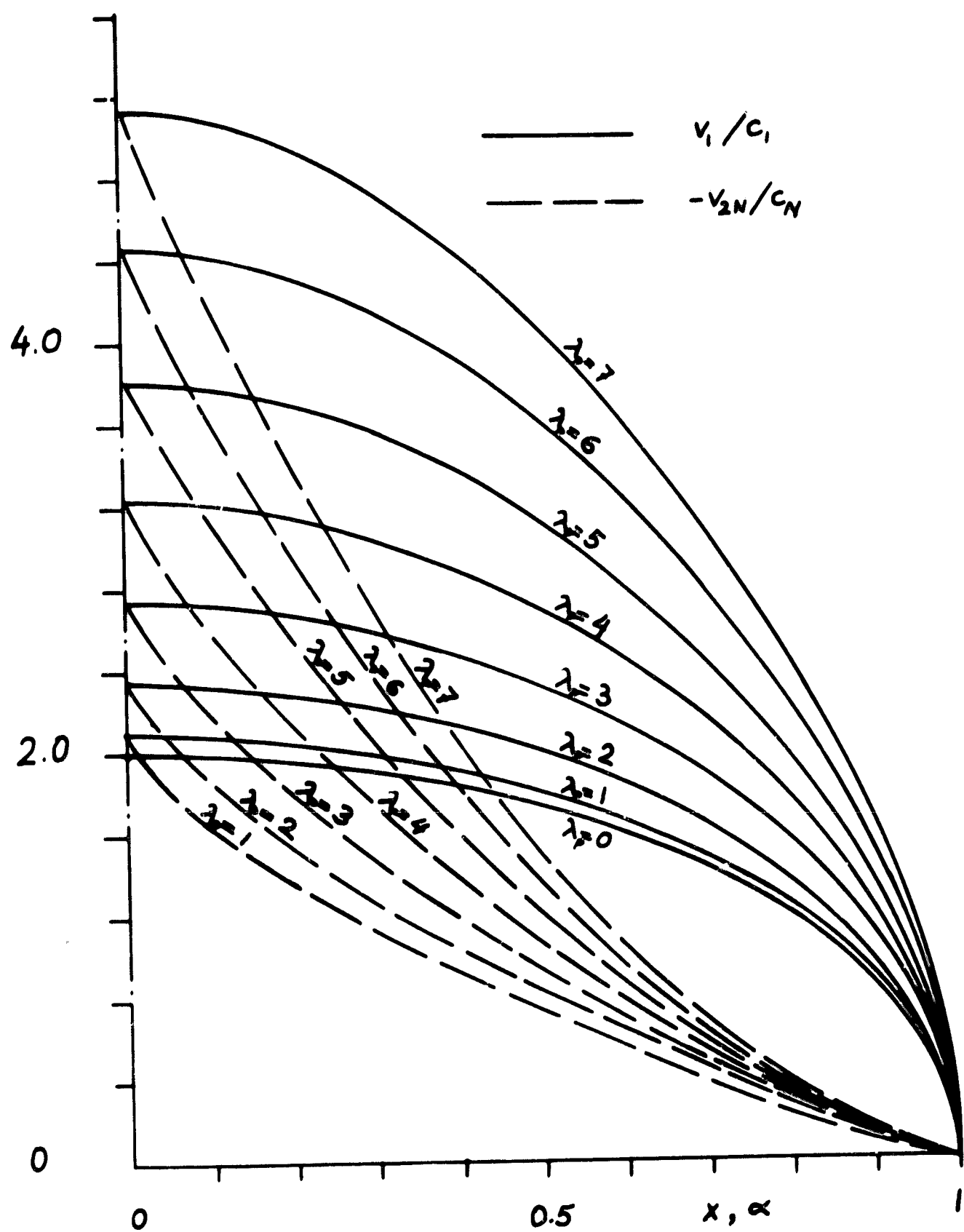
Figure 7. Crack surface displacements in cylindrical shells with a circumferential crack under membrane loads.
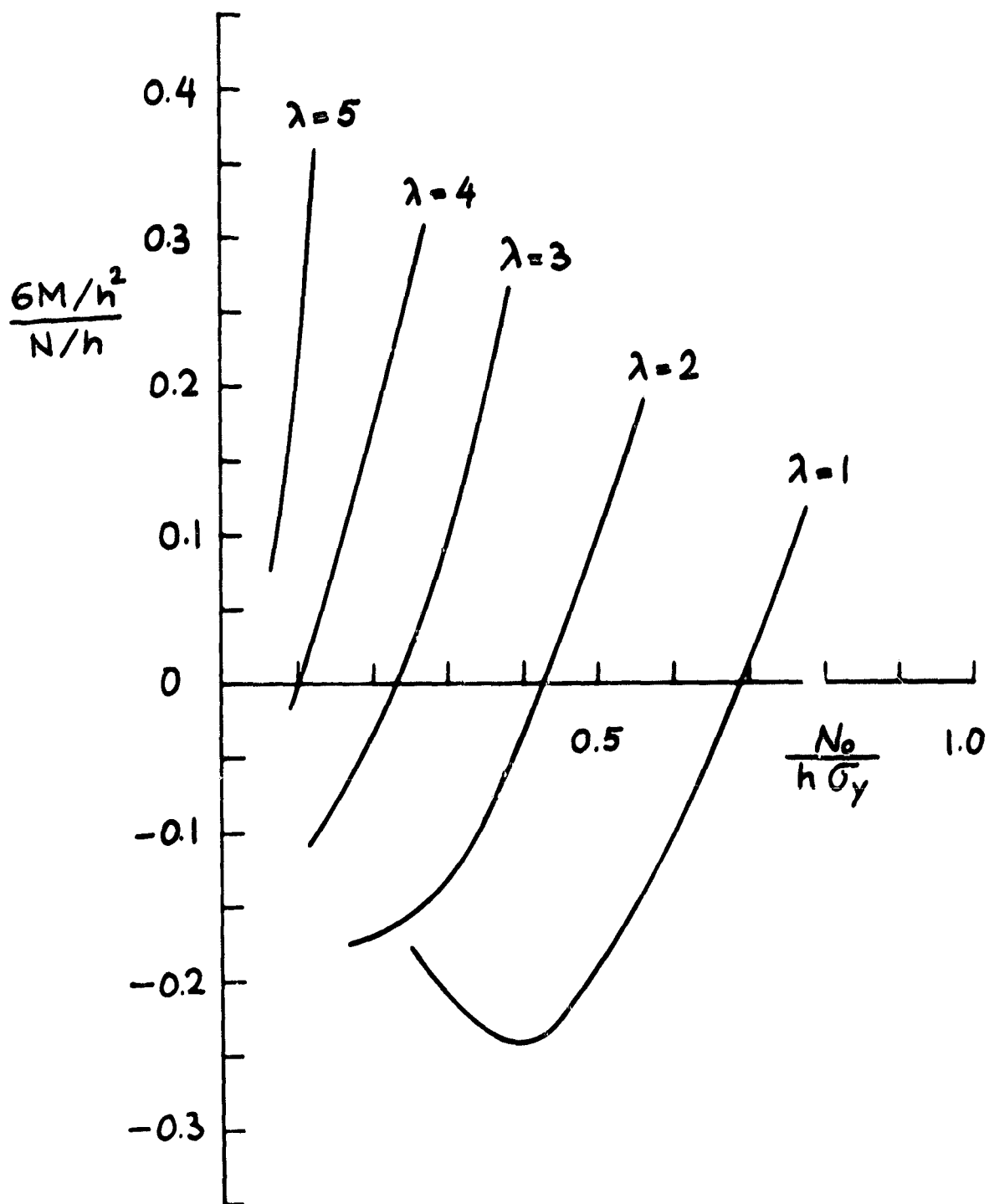
Figure 8. Bending-to-membrane stress ratio in the plastic strip in cylindrical shells with an axial crack.
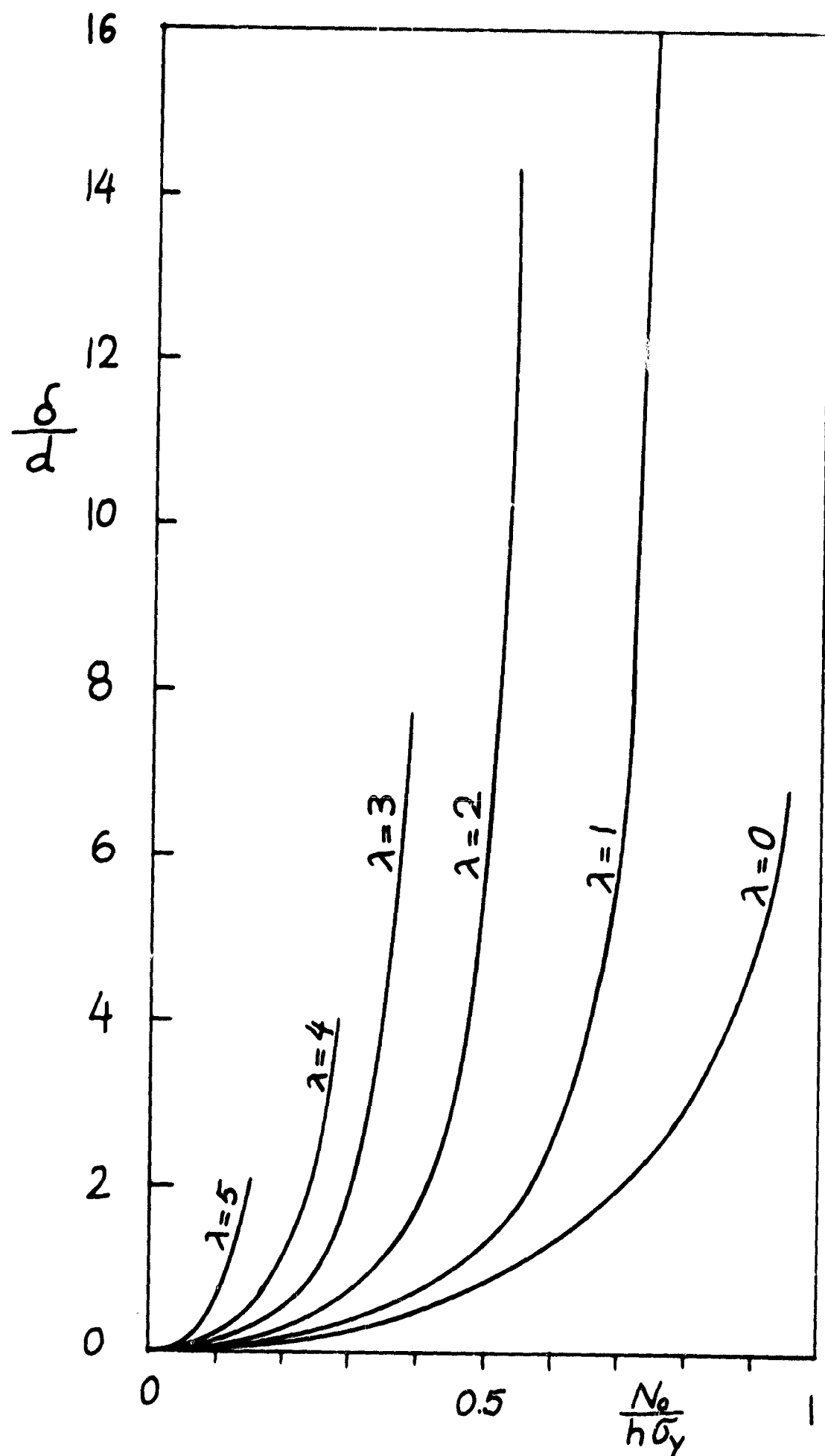
Figure 9. Crack opening displacement in cylindrical shells with an axial crack.
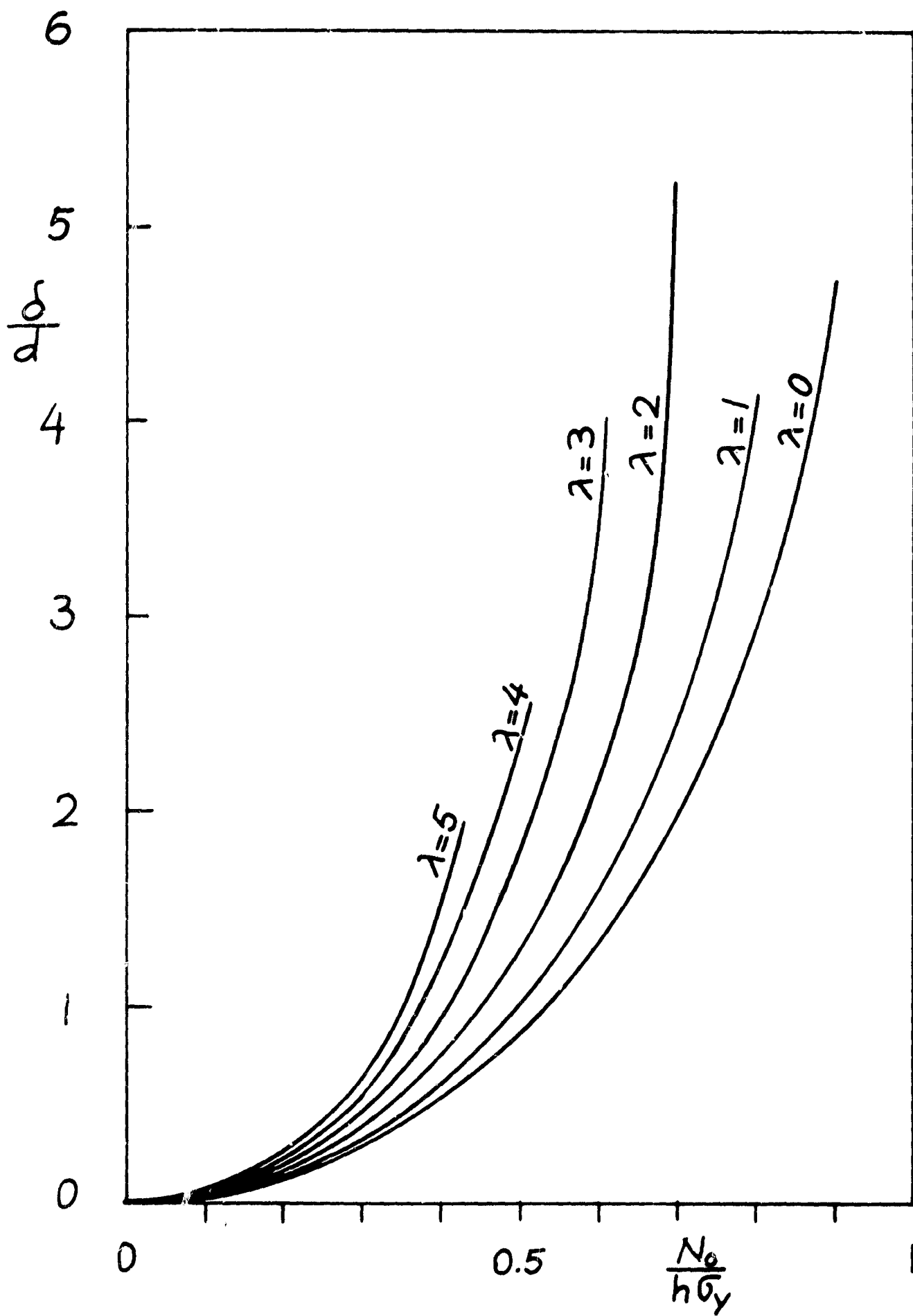
Figure 10. Crack opening displacement in cylindrical shells
with a circumferential crack.
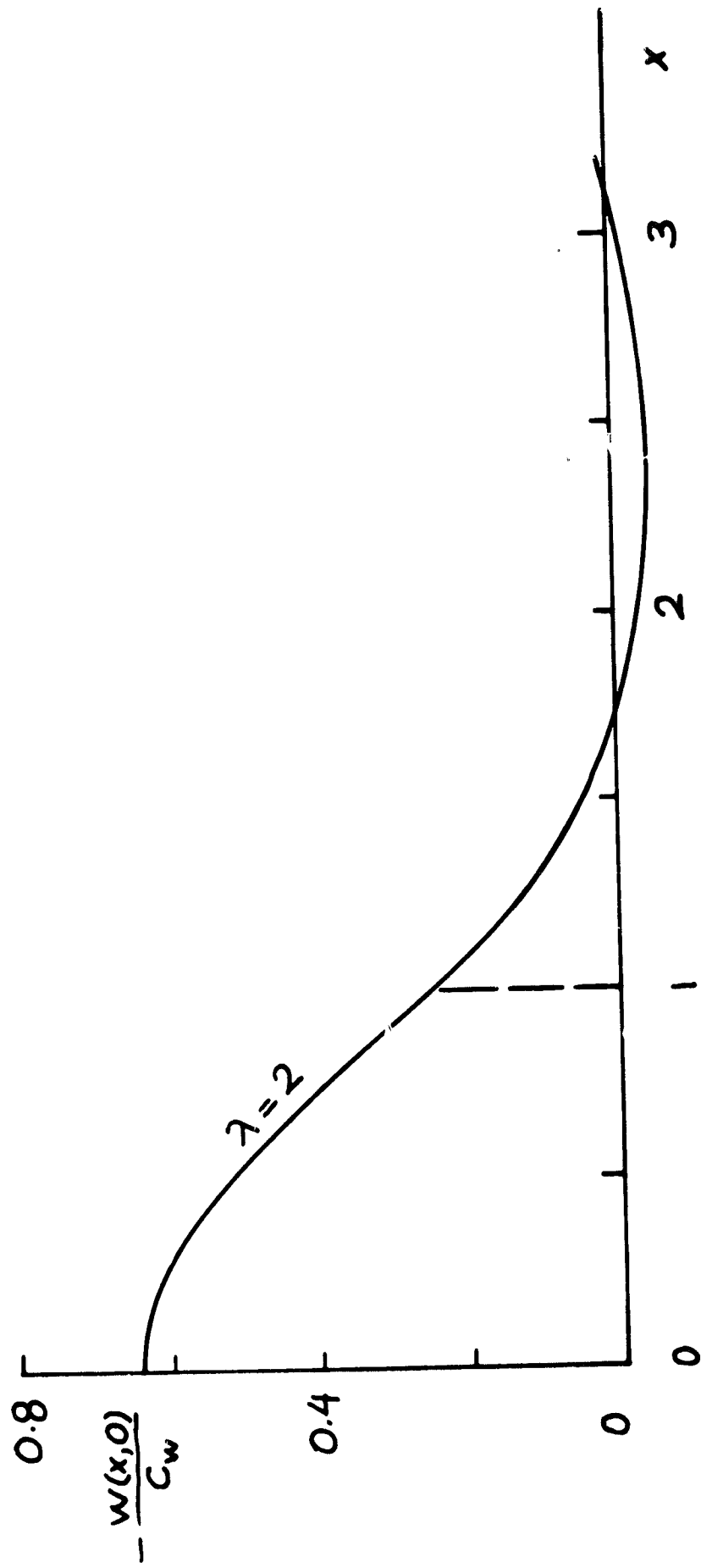
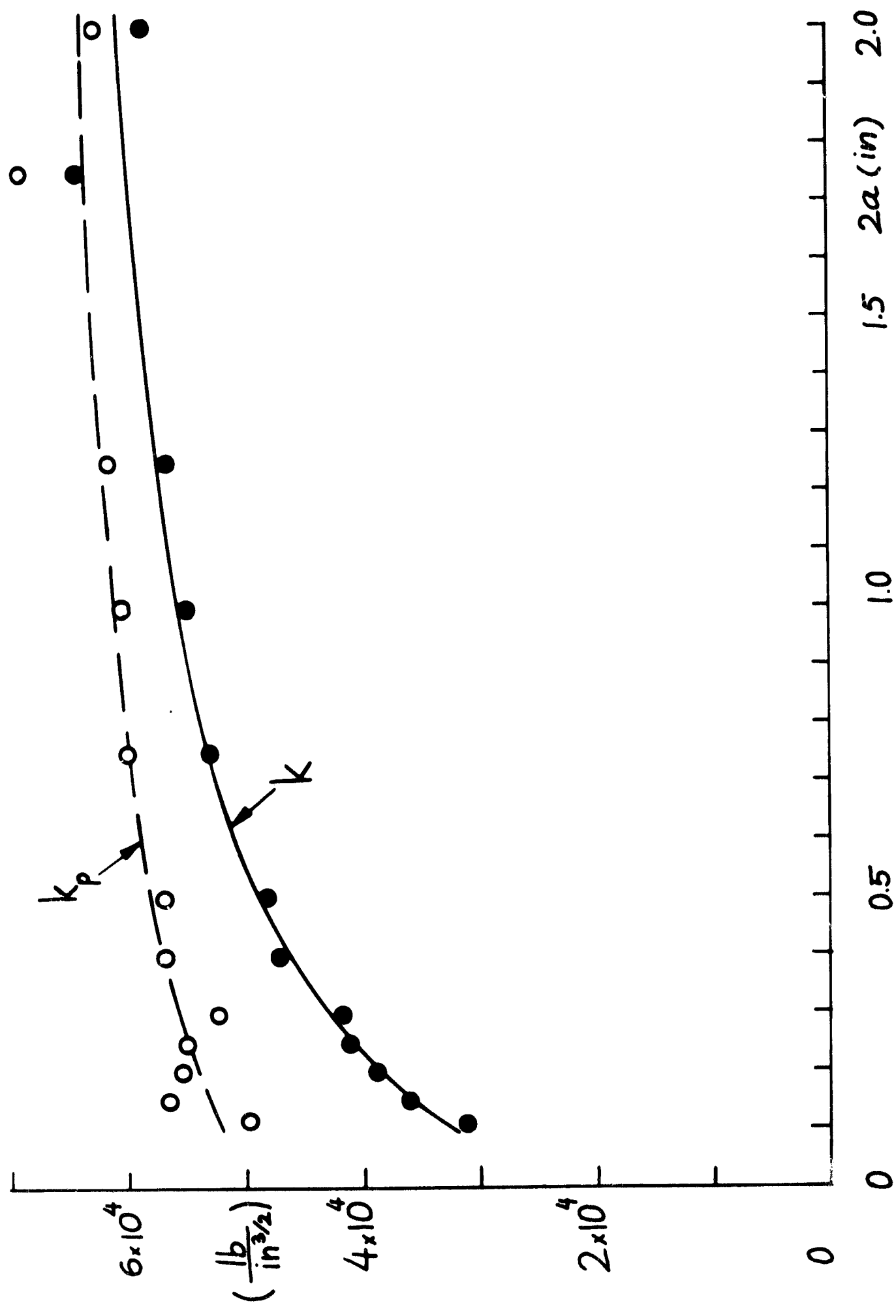Figure 11. Normal displacement at the crack surface in a cy-
lindrical shell.

Figure 12. k and k_p in 2014-T6 aluminum cylinders tested at -320°F.
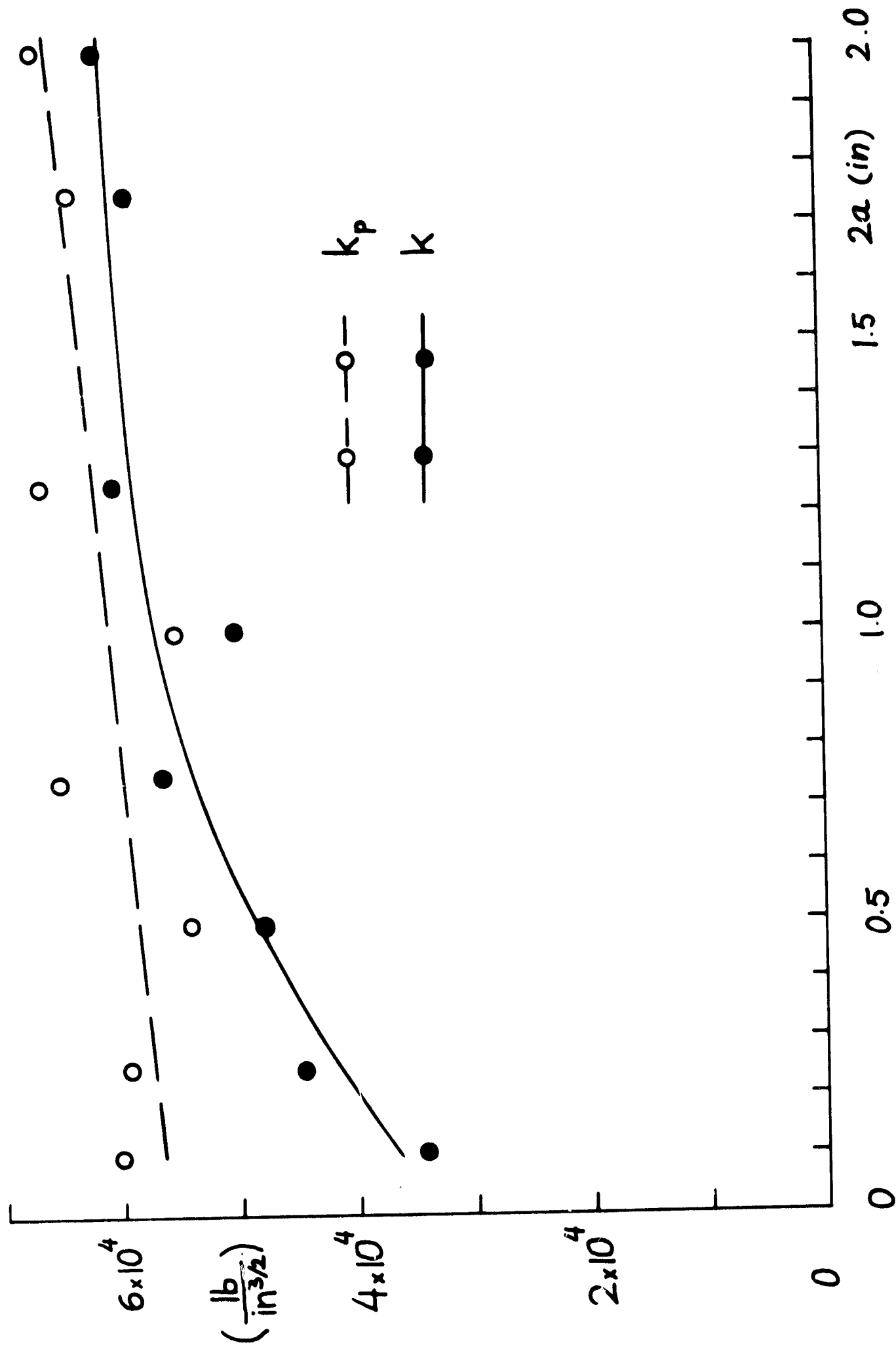
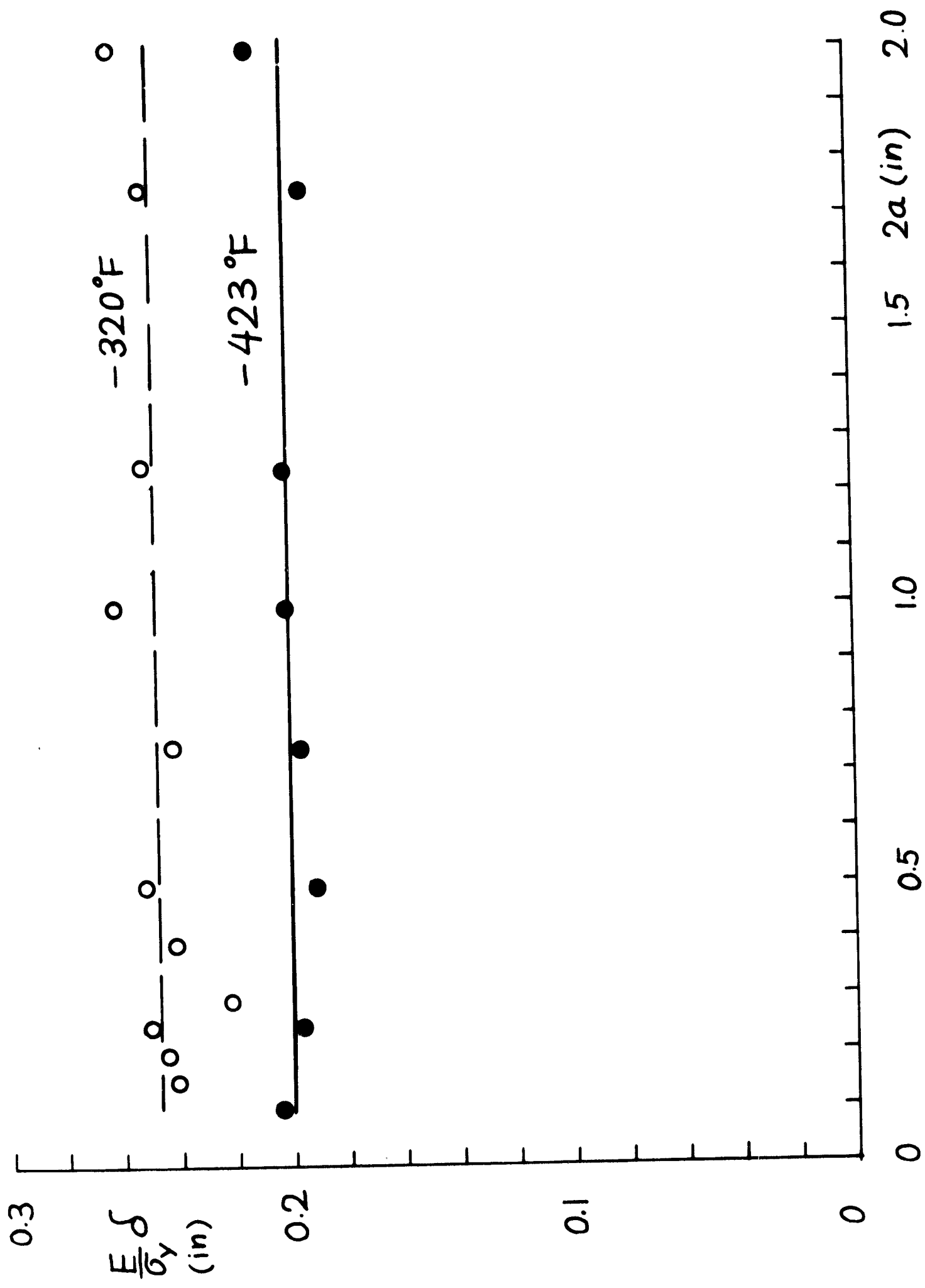Figure 13. k and k_p in 2014-T6 aluminum cylinders tested at -423°F.

Figure 14. Crack opening displacement in 2014-T6 aluminum cylinders tested at -320°F and -423°F.